Investigation on the pressure drop during flow boiling of liquefied natural gas in a vertical micro-fin tube

Xu Bin Shi Yumei
(Inst. of Refrigeration and Cryogenics Eng., Shanghai Jiaotong Univ., Shanghai, China 200240)

Abstract: This paper presented an experimental investigation on the pressure drop during flow boiling of liquefied natural gas in a vertical micro-fin tube. The effect of heat flux, mass flux and inlet pressure on the frictional pressure drop during two-phase flow of liquefied natural gas was analyzed. Results showed that the two-phase flow pressure drop increased with the increasing of heat flux and mass flux but decreased with the increasing of inlet pressure. The calculated results with Miyara correlation, Oliver correlation, Hu correlation and Goto correlation showed that the Hu correlation could give the best prediction which also has a big error. Thence a new correlation was developed based on the experimental data.

Keywords: Flow boiling Liquid nitrogen Two-phase flow Pressure drop

0. Introduction

Coal, oil and natural gas (NG) are three kinds of most important primary energy in the world today. And in the current decades, the NG becomes more and more important since it is clean, efficient and economical. The NG is more and more widely used in industrial production, transportation, and other civilian fields. To improve the storage efficiency, especially to save the storage space on the ship when transported by sea, NG is typically stored and transported in the form of liquefied natural gas(LNG) after impurities are removed[1]. Finally, the LNG should be utilized in the form of natural gas at room temperature after vaporization. So in the natural gas liquefaction and LNG gasification process, we need to optimize the design of the heat exchanger in order to improve energy efficiency as well as for the economic considerations. And it's very necessary to figure out the frictional pressure drop characteristics during flow boiling of liquid natural gas in tubes for the design of the heat exchanger[2].

Very few research papers about the flow boiling of the liquefied natural gas in a tube could be found among the published literature although the research of the two-phase flow boiling has been conducted for several decades since the 1960s as we know. There is also very little research on flow boiling of the cryogenic fluid in enhanced tubes. Currently, the studies on the flow boiling in enhanced tubes are mainly about water or refrigerants which are liquid at room temperature. M.Balcilar[3]et al. have done numerical study on the flow boiling of R32, R125, R22 and the mixture of R32 and R134a in several different horizontal smooth tubes and micro-fin tubes. And they found that the pressure drop of the flow boiling is closely related with the mass flow rate, total liquid Reynolds, latent heat of vaporization and the dryness of the outlet. Kim[4]et al. have taken experimental research on the heat transfer and pressure drop characteristics during flow boiling of R22 in smooth tubes and micro-fin tubes with the length of 3m and they have evaluated the heat transfer enhancement effect in micro-fin tubes compared with in smooth ones. Hu[5]et al. experimentally investigated the frictional pressure drop characteristics during flow boiling of the mixture of R410A-oil in a straight enhanced tube and a C-shaped enhanced tube. And they developed a new correlation to predict the pressure drop based on the properties of the mixture.

This paper presents an experimental investigation on the pressure drop characteristics of LNG flow boiling in a vertical micro-fin tube. The effect of heat flux, mass flux and inlet pressure on the flow boiling pressure drop coefficients was analyzed. The Miyara, Oliver, Hu and Goto correlations were adopted to predict the flow boiling pressure drop coefficients and the results predicted by different correlations were compared with the experimental data to find out the most accurate correlation.

1. Experimental apparatus

The test set-up was designed to measure the local heat transfer coefficient and pressure drop of the LNG flowing through the test tube. Fig.1 illustrates the schematic diagram of the experimental apparatus. The test set-up mainly consisted of the LNG flow loop, vacuum Dewar and signal acquisition system. LNG in the storage tank with a capacity of 500L and adjustable operating pressure of 0.1~1.6MPa was supplied to the test section after it is precooled in the liquid nitrogen container. LNG from the outlet of the test section was completely vaporized in the vaporizer and then flowed through the mass flow meter to measure the mass flow rate. The vaporized LNG flowed into the environment finally. The temperature and pressure of each test point and the voltage and current signals of the DC power supplier were tested and collected by the data acquisition instrument while the mass flow rate was directly measured by the mass flow meter and the results were stored in the computer.

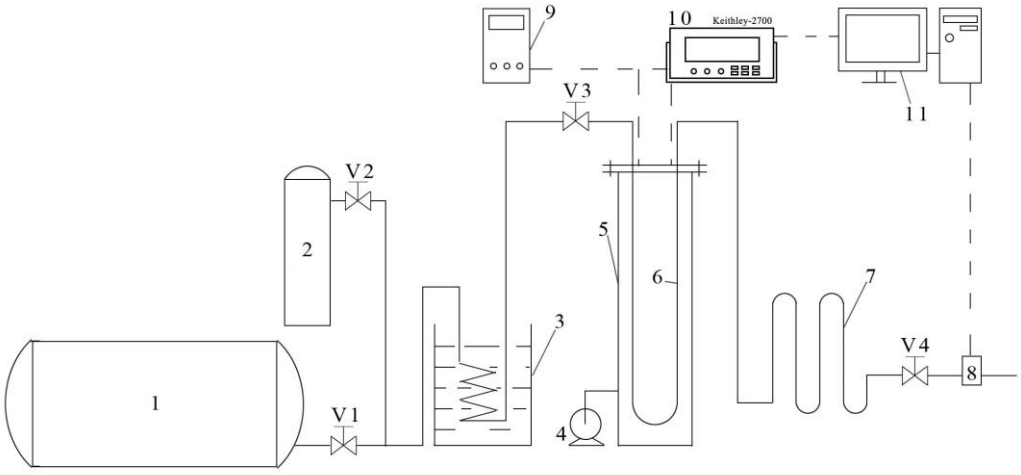

Fig.1 System Diagram of experimental apparatus

1.LNG storage tank 2.Nitrogen gas cylinder 3.Liquid nitrogen container 4.Vacuum pump 5.Vacuum dewar 6.Test section 7.Vaporizer 8.Mass flow meter 9.DC power controller 10.Data acquisition instrument 11.Computer V1-V4.Valves

Fig.2 illustrates the schematic diagram of test section. 12 platinum resistance temperature sensors were installed symmetrically on 6 different test cross-sections which were distributed evenly on the test section. Moreover, one more platinum resistance temperature senor was installed nearby the outlet of the test section to measure the wall temperature of outlet and an inlet temperature sink hole was designed before the inlet of the test section to get the inlet temperature of the LNG flowing in the tube. As Fig.3 shows, the test section was a micro-fin vertical copper tube with an effective heating length of 1000mm and outer diameter of 12.7mm. The electric heating wire was evenly wounded over the test section and thermal conductive silicone was used to ensure that the LNG would be heating evenly. Wool felt and aluminum foil were covered over the electric heating wire successively and the whole test section was placed in a vacuum Dewar to reduce heat leakage. Fig.4 shows the structure of the micro-fin tube and the geometric details of the micro-fin tube are listed in Table 1.

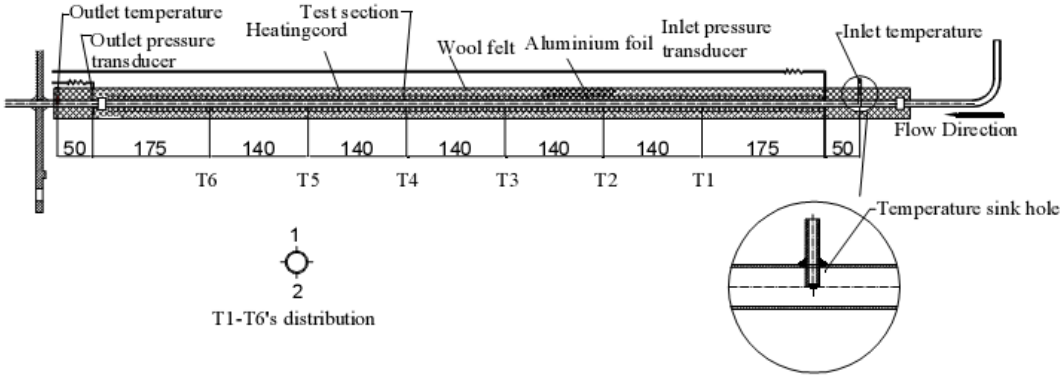

Fig.2 Schematic diagram of test section

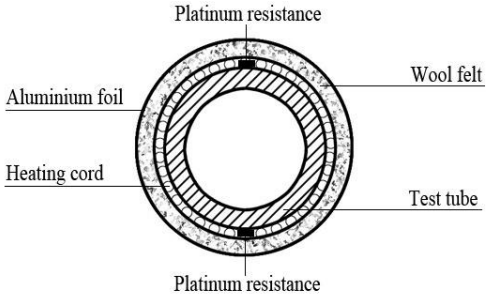

Fig.3 Schematic diagram of test tube cross-section

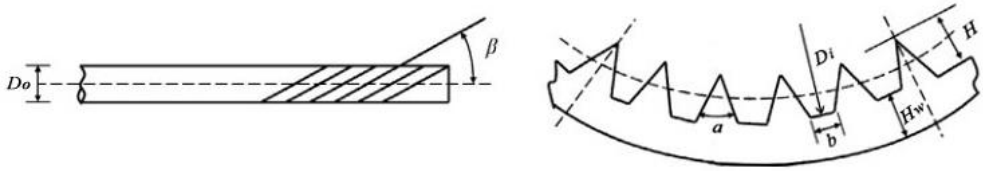

Fig.4 Schematic diagram of the micro-fin tube's structure

Table 1 Geometries of the micro-fin tube

Parameter	Value
Outer diameter, D_o	12.7mm
Inner diameter, D_i	11.8mm
Number of fins, N	60
Fin root thickness, H_w	0.457mm
Fin height, H	0.254mm
Fin pitch, b	0.617mm
Apex angle, α	40^o
Helix angle, β	18^o

2. Experimental study

2.1 Data measurement and uncertainty analysis

The main measured parameters involve the inlet pressure of the test tube, the pressure difference between inlet and outlet of the test tube, the mass flow rate of the LNG, the wall temperatures of 7 different cross-sections along the flowing direction, the LNG temperature at the entrance, and the electric voltage and current of the power supply.

The uncertainties in experiments were calculated using the guidelines suggested by NIST[7] and the main experimental uncertainties are listed in Table 2.

Table 2 Summary of the uncertainty analysis

Parameter	Uncertainty
Diameter, D (mm)	±0.001
Length, L (mm)	±1.0
Temperature, T (K)	±0.1
Pressure, P (kPa)	±4.0
Pressure difference ,ΔP (kPa)	±0.175
Mass flow rate ,(%)	±0.8
Mass flux, G (%)	±0.9
Heat flux, q (%)	±4.1

2.2 Experimental conditions

There were 96 different operating conditions experimentally achieved in which the inlet pressure, the mass flow rate and the heat flux varied from 0.3 to 0.9MPa, 24.91 to 99.62kg/(m^2s) and 5.05~25.18kW/m^2 respectively.

2.3 Data reduction

Heat flux is determined by the electric voltage and current through the electric heating wire.

$$Q = UI \tag{1}$$

$$q = \frac{Q}{A_s} \tag{2}$$

$$A_s = \pi D l \tag{3}$$

The physical parameters of the LNG on each test cross-section, such as $T_{f,z}$, vapor quality, viscosity, the percentage of vapor phase and so on, were calculated according to the phase equilibrium of mixture and the principle of the thermal balance with choosing the Peng-Robinson equation of state. The pressure at each test cross-section was calculated by linear interpolation between inlet pressure P_{in} and outlet pressure P_{out} of the test section as the inlet pressure and the pressure difference between inlet and outlet were measured. The compositions of the LNG used in experiments are listed in Table 3, which were supplied by Shanghai Nature Gas Pipeline Network Co., Ltd.

Table 3 Composition of LNG

Composition	Methane	Ethane	Propane	i-butane	n-butane	nitrogen
Mole Fraction(%)	0.8969	0.0602	0.0307	0.0063	0.0057	0.0002

The pressure drop consists of frictional pressure drop, gravity pressure drop and acceleration pressure drop during flow boiling of the LNG in a vertical micro-fin tube.

$$\Delta p = \Delta p_f + \Delta p_g + \Delta p_a \tag{4}$$

Considering the test section was evenly heated, the quality distributed linearly in the flow direction. The gravity pressure drop and acceleration pressure drop during flow boiling of LNG in a vertical tube could be calculated by the formulas below which were deduced according to the gas-liquid two-phase flow momentum equations.

$$\Delta p_g = \frac{gl}{x_{out}} \int_{x_{in}}^{x_{out}} [(1-\alpha)\rho_L + \alpha\rho_G] dx \tag{5}$$

$$\Delta p_a = G^2 \left[\frac{(1-x_{out})^2}{\rho_L (1-\alpha_{out})} + \frac{x_{out}^2}{\rho_G \alpha_{out}} - \frac{1}{\rho_L} \right] \tag{6}$$

Where the void fraction was calculated according to minimum entropy model[6]:

$$\alpha = \left[1 + \left(\frac{1-x}{x} \right) \left(\frac{\rho_L}{\rho_G} \right)^{2/3} \right]^{-1} \tag{7}$$

3 Analysis of two-phase flow frictional pressure drop

Mass flux and heat flux both have significant impact on the two-phase flow frictional pressure drop. Experimental values of two-phase flow frictional pressure drop could be calculated by equation (8), which was converted from equation (4).

$$\Delta p_f = \Delta p - \Delta p_g - \Delta p_a \tag{8}$$

Where the gravity pressure drop and acceleration pressure drop were calculated by the equation (5),(6) respectively.

3.1 Effect of heat flux

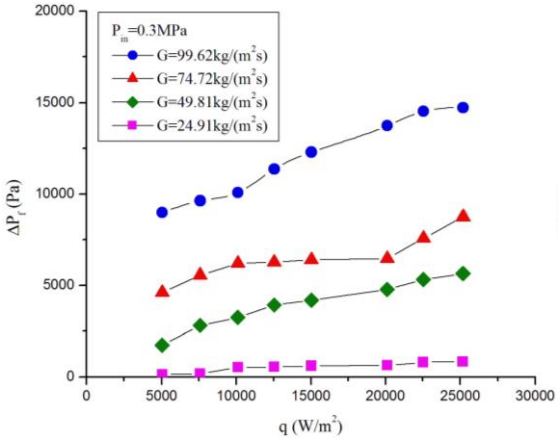

(a) P_{in}=0.3MPa, G=24.9-99.62kg/(m^2s)

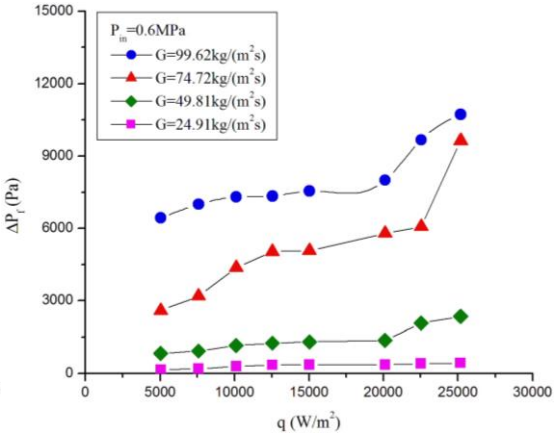

(b) P_{in}=0.6MPa, G=24.9-99.62kg/(m^2s)

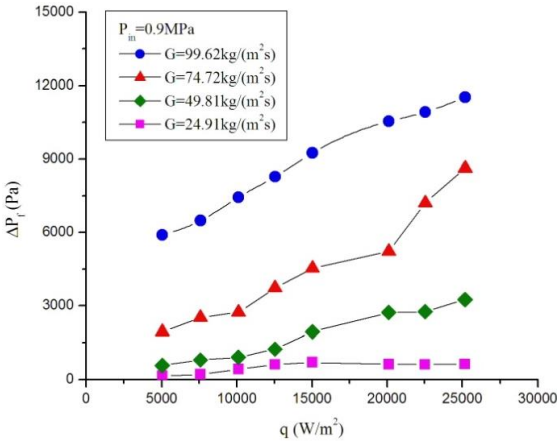

(c) P_{in}=0.9MPa, G=24.9-99.62kg/(m^2s)

Fig.5 Effect of heat flux on the two-phase flow frictional pressure drop

Fig.5(a), (b) and (c) show the effect of heat flux on two-phase flow frictional pressure drop at eight different heat fluxes while the inlet pressure was 0.3MPa, 0.6MPa and 0.9MPa, and the mass fluxes varied from 24.91kg/(m^2s) to 99.62kg/(m^2s). The result shows that the two-phase flow frictional pressure drop increased with the heat flux while the mass flux and the inlet pressure keep the same. And the trend of the frictional pressure drop's increasing with the heat flux was more obvious under the greater mass fluxes just as G=99.62kg/(m^2s) and G=74.72kg/(m^2s). According to the mechanism of flow boiling heat transfer and pressure drop, the vapor fraction of the LNG flowing in the test tube increased with the heat flux, and this enhanced the interaction between the liquid and vapor phases, and as a result, the frictional pressure drop increased.

3.2 Effect of mass flux

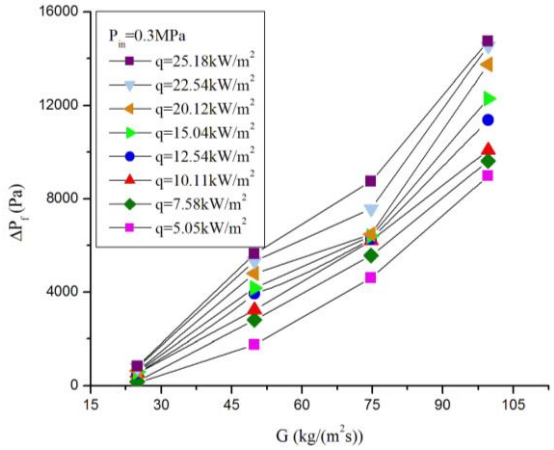

(a) (a) P_{in}=0.3MPa, q=5.05-25.18kW/m^2

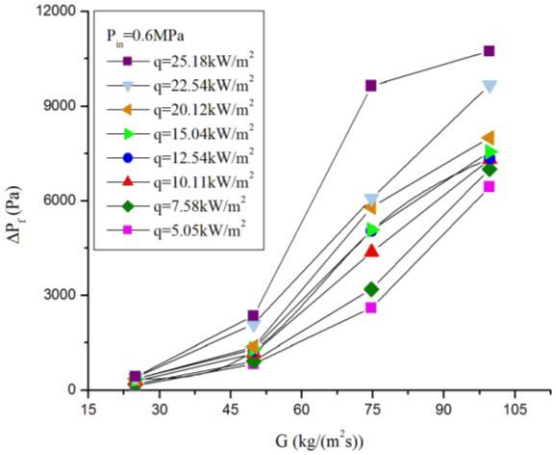

(b) P_{in}=0.6MPa, q=5.05-25.18kW/m^2

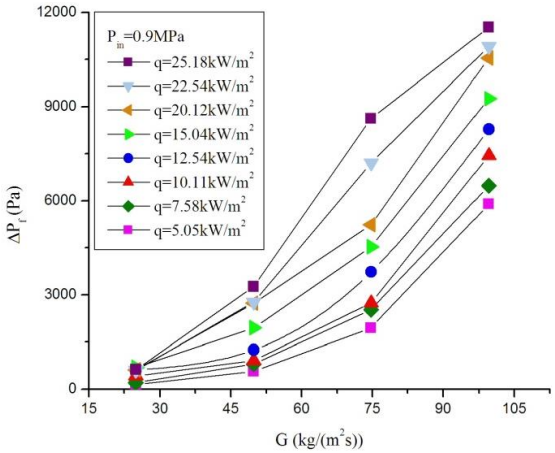

(c)P_{in}=0.9MPa, q=5.05-25.18kW/m^2

Fig.6 Effect of mass flux on the two-phase flow frictional pressure drop

Fig.6 (a), (b) and (c) show the frictional pressure drop's variety with different mass fluxes in the condition of eight different heat fluxes with the inlet pressure of 0.3MPa, 0.6MPa and 0.9MPa respectively. The result shows that the two-phase flow frictional pressure drop increased with the mass flux. According to both the theory of phase separation model and homogeneous model of two-phase flow boiling, the frictional pressure is proportional to the square of the mass flow or the velocity of the LNG flowing in the test tube. Therefore the two-phase flow boiling frictional pressure drop increased with the mass flux.

3.3 Effect of inlet pressure

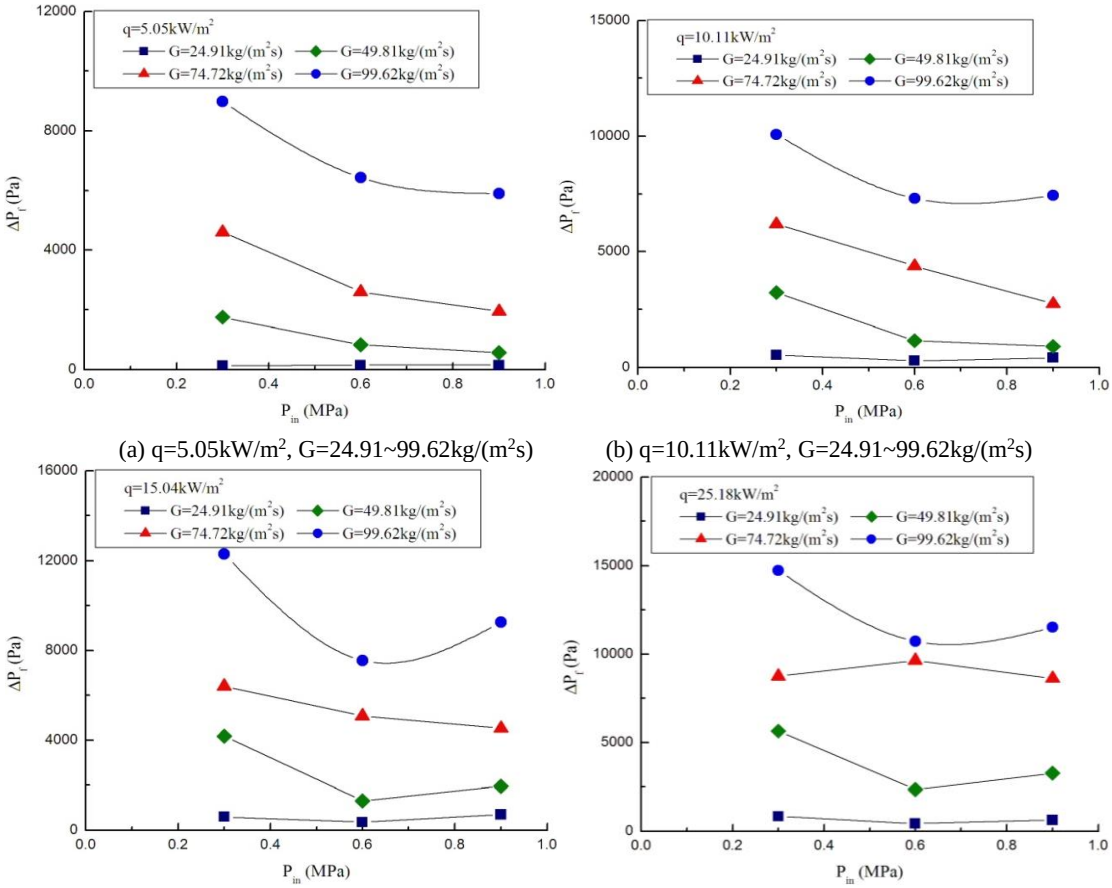

(a) q=5.05kW/m^2, G=24.91~99.62kg/(m^{2}s) (b) q=10.11kW/m^2, G=24.91~99.62kg/(m^{2}s)

(c) q=15.04kW/m^2, G=24.91~99.62kg/(m^{2}s) (d) q=25.18kW/m^2, G=24.91~99.62kg/(m^{2}s)

Fig.7 Effect of inlet pressure on the frictional pressure drop

Fig.7 (a), (b) and (c) show the frictional pressure drop's variety with different inlet pressures in the condition of four different mass fluxes while the heat fluxes varied from 5.05kW/m^2 to

25.18kW/m^2. The result shows that the two-phase flow frictional pressure drop decreases with the inlet pressure. The probable reason is that the density of the vapor phase increased with the system pressure over the whole test section while the density of the liquid phase had little change, and on the other hand, the pressure drop during the two phase flow boiling was so little compared to the inlet pressure that we could assumed that the system pressure over the whole test section was the same as the inlet pressure. As a result, the average density of LNG in the test tube increased with the inlet pressure and the velocity of the LNG decreased with the inlet pressure when the mass flow rate kept the same. Finally the two-phase flow boiling frictional pressure drop decreased with the inlet pressure.

4. Correlations calculation

There was no satisfactory theoretical explanation for the mechanism of the flow boiling in enhanced tubes just for its complexity. And the former research was mainly based on the theory of semi-theoretical and semi-empirical correlation. In this paper, the Miyara[7][8], Oliver[9], Hu[5] and Goto[10] correlations were used to predict the two-phase flow boiling frictional pressure drop. The results predicted by different correlations were compared with the experimental data and the errors of the four correlations were calculated in order to analyze the accuracy of the different correlations.

4.1 Frictional pressure drop correlations

In previous studies, the working fluid flowing in the enhanced tubes were mostly refrigerants or water known as the conventional fluid. All the correlations mentioned in this paper are listed in Table 4.

Table 4 Flow boiling frictional pressure drop correlation

Correlation's name	Frictional pressure drop
Miyara[7][8]	$\left(-\frac{dP_f}{dz}\right)=\phi_G^2\frac{2f_G(Gx)^2}{\rho_G D_i}$ *where,* $f_G=0.046\,\mathrm{Re}_G^{-0.2},\ \mathrm{Re}_G=GxD_i/\mu_G,\ \varphi_G=1.2+1.65(FrX)^{0.35}$ $Fr=\frac{G}{\sqrt{\rho_G(\rho_L-\rho_G)gD_i}}$ $X=\left(\frac{1-x}{x}\right)^{0.9}\left(\frac{\rho_G}{\rho_L}\right)^{0.5}\left(\frac{\mu_L}{\mu_G}\right)^{0.1}$
Oliver[9]	$\left(-\frac{dP_f}{dz}\right)=\varphi_L^2\frac{2f_L(G(1-x))^2}{\rho_L D_i}$ *where,* $f_L=0.046\,\mathrm{Re}_L^{-0.2}\left(\frac{D_n}{D_i}\right)\left(\frac{A}{A_n}\right)^{0.5}(2\sec\beta)^{1.1}$ $\frac{A}{A_n}=1-\frac{2hnt}{\pi D_n^2\cos\beta}$ $\mathrm{Re}_L=G(1-x)D_i/\mu_L$ $\varphi_L{}^2=1.376+\frac{7.242}{X^{1.655}},\ X=\left(\frac{1-x}{x}\right)^{0.9}\left(\frac{\rho_G}{\rho_L}\right)^{0.5}\left(\frac{\mu_L}{\mu_G}\right)^{0.1}$
Hu[3][5]	$P_f=\varphi_G^2\frac{2f_G(Gx)^2}{\rho_G D_i}L$ *where,* $f_G=0.051\,\mathrm{Re}_G^{-0.06},\ \mathrm{Re}_G=GxD_i/\mu_G,\ \varphi_G=1+3.74X^{0.586}$ $X=\left(\frac{1-x}{x}\right)^{0.9}\left(\frac{\rho_G}{\rho_L}\right)^{0.5}\left(\frac{\mu_L}{\mu_G}\right)^{0.1}$

	$\left(-\frac{dP_f}{dz}\right)=\varphi_G^2\frac{2f_G(Gx)^2}{\rho_G D_i}$ *where,* $\varphi_G=1+1.64X^{0.79}$
Goto[10]	$f_G=\begin{cases}2.17\times10^{-2}\,\mathrm{Re}_G^{-0.08} & ,\mathrm{Re}_G<3900\\ 1.10\times10^{-3}\,\mathrm{Re}_G^{0.28} & ,3900\le\mathrm{Re}_G\le11500\\ 1.53\times10^{-2} & ,11500<\mathrm{Re}_G\end{cases}$ $X=\left(\frac{1-x}{x}\right)^{0.9}\left(\frac{\rho_G}{\rho_L}\right)^{0.5}\left(\frac{\mu_L}{\mu_G}\right)^{0.1}$

4.2 Comparison of experimental results with calculations by existing correlations

As Fig.8 shows, we compared 96 sets of experimental data with the results calculated by four different correlations. And the experiment were conducted at inlet pressure from 0.3to 0.9MPa, with the heat flux of 5.05~25.18kW/m^2 and the mass flux of 24.91~112.1kg/(m^{2}s).

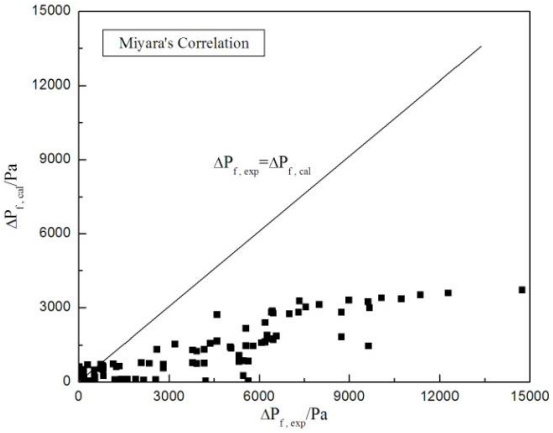

Fig.8-1 Miyara's correlation compared with the experimental data

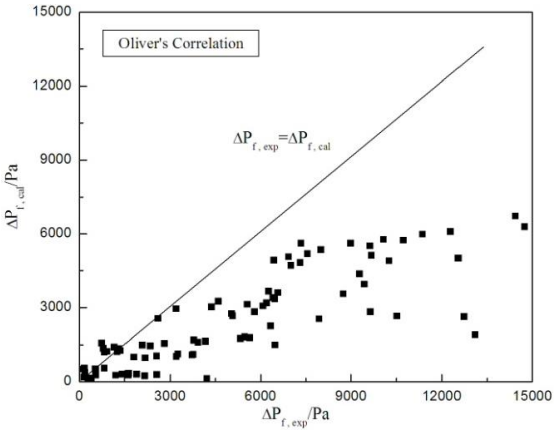

Fig.8-2 Oliver's correlation compared with the experimental data

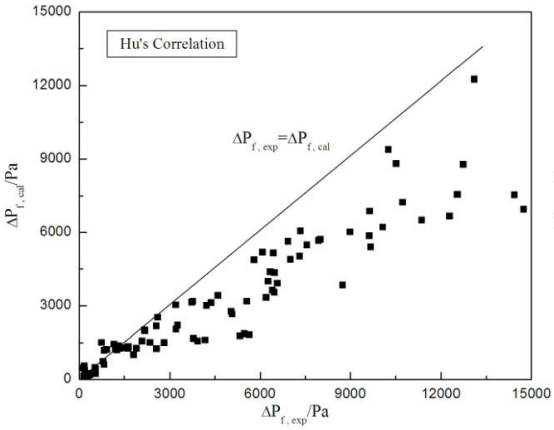

Fig.8-3 Hu's correlation compared with the experimental data

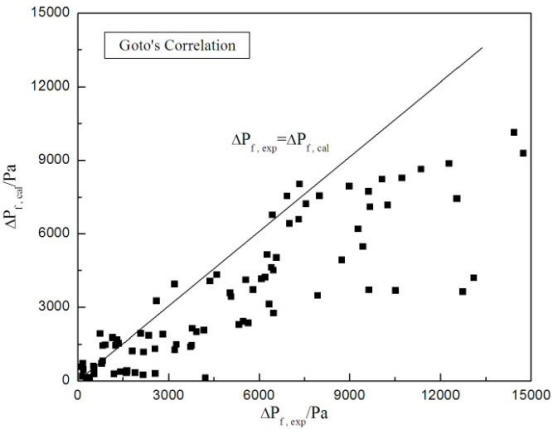

Fig.8-4 Goto's correlation compared with the experimental data

Fig.8 Experimental frictional pressure drop compared with calculated results using correlations

Table 5 Deviation between the predicted HTC and the experimental data

Correlations	AAD(%)	RMS(%)
Miyara	68.7	73.3
Oliver	34.9	69.2
Hu	19.5	54.2
Goto	21.6	65.7

AAD: Absolute Average of Deviation; RMS: Root Mean Square of Deviation

Table 5 lists the deviations between the experimental data and the results predicted by four different correlations. The result shows that Hu correlation was the most accurate in the range of the experimental conditions with the absolute average of deviation of 19.5% and root mean square of deviation of 54.2% which are both the minimum of the four different correlations. In addition, it also could be seen that all values of the frictional pressure drop predicted by the four correlations are smaller than the experimental results. And the larger the frictional pressure drop was, the more the values predicted by correlations deviated from the experimental results.

4.3 Development of new correlation

Considering that large deviation exists between the experimental results and the values predicted by the four correlations, we developed a new correlation by amending the φ_c coefficient in the Hu correlation which was the most accurate in the four correlations chosen based on the experimental data. And the new φ_c coefficient is as follows.

$$\varphi_G = 1 + 5.76X^{0.352} \tag{9}$$

Fig.9 shows the comparison between the experimental results and the values predicted by the new correlation. And the absolute average of deviation is 5.3% while the root mean square of deviation is 24.6%.

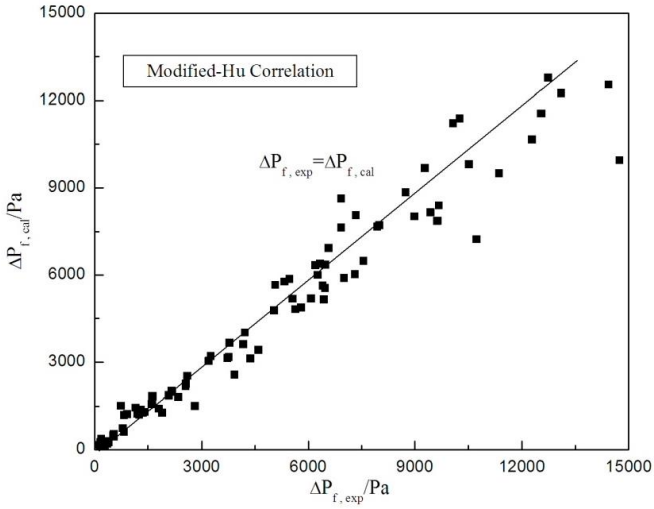

Fig.9 Experimental frictional pressure drop compared with the predicted value of modified-Hu correlations

5. Conclusion

(1) This paper presents an experimental investigation on the pressure drop characteristics of liquefied natural gas flow boiling in a vertical micro-fin tube. The effect of heat flux, mass flux and inlet pressure on the frictional pressure drop during two-phase flow of liquefied natural gas was analyzed. And the result shows that the two-phase flow boiling frictional pressure drop increased with both the mass flux and the heat flux but decreased with the inlet pressure.

(2) Four correlations were adopted to predict the frictional pressure drop for comparison with the experimental data including Miyara, Oliver, Hu and Goto correlations. The result showed that the Hu correlation is the most accurate over the whole experimental conditions as its AAD and RMS are 19.5% and 54.2% respectively, which are both the minimum of the 4 correlations.

(3) Considering that results predicted by the four correlations were not satisfactory, a new correlation was developed by amending the φ_c coefficient in Hu correlation based on the the experimental data. The AAD and RMS of the new correlation are 5.3% and 24.6% respectively.

Nomenclature

U	——	Voltage，V	h_{lv}	——	Latent heat of vaporization，J kg^{-1}
I	——	Current，A	x	——	Quality
Q	——	Heating Power，W	z	——	Coordinate
q	——	Heat Flux，W m^{-2}	λ	——	Thermal conductivity，W m^{-1} K^{-1}
A_c	——	Cross-sectional area，m^2	Re	——	Reynolds number
A_s	——	Effective heating area、，m^2	Pr	——	Prandtl number
P	——	Pressure，Pa	X	——	Martinelli parameter
T	——	Temperature，K	M	——	Molecular weight
μ	——	Dynamic viscosity，pa s^{-1}	h	——	Local heat transfer coefficient
ρ	——	Density，kg m^{-3}	α	——	Void fraction
L	——	Length of the test section，m	f	——	Frictional factor
G	——	Mass flux，kg s^{-1}	φ_G	——	Gas phase frictional multiplier
D_i，D_o	——	Inner diameter and outer diameter respectively，m	φ_L	——	Liquid phase frictional multiplier

Subscripts

in	——	Inner	*G*	——	Gas
out	——	Outer	*L*	——	Liquid

References

[1] Anzhong Gu. LNG Technical Manual[M]. Machinery Industry Press, 2010.1.1, 1-5.

[2]Hu Haitao, Ding Guoliang et al. The Frictional Pressure Drop Characteristics of R410A-Oil Mixture Flow Boiling inside a φ7 mm Horizontal Straight Smooth Tube[J]. Journal of Shanghai Jiaotong University, 2007, 41(3):370-375.

[3]M.Balcilar. A correlation development for predicting the pressure drop of various refrigerants during condensation and evaporation in horizontal smooth and micro-fin tubes[J]. International Communications in Heat and Mass Transfer, 2012, 39:937-944.

[4]K.Seo, Y.Kim. Evaporation heat transfer and pressure drop of R-22 in 7 and 9.52mm smooth/micro-fin tubes[J]. International Journal of Heat and Mass Transfer, 2000, 43:2869-2882.

[5]Hu Haitao et al. Frictional pressure drop characteristics of R410A-oil mixture flow boiling in 7 mm straight and C-shape enhanced tubes[J]. Journal of Chemical Industry and Engineering (China), 2007, 58(8):1905-1910.

[6]Zivi, S. Estimation of steady-state steam void-fraction by means of the principle of minimum entropy production[J]. Journal of Heat Transfer, 1964, 86(247): p2.

[7]Miyara, A., Otsubo, Y. Evaporation heat transfer of R410A in herringbone micro-fin tubes. Conf. IIR Commission B1 2001/5, Thermophysical physical properties and transfer process of new refrigerant. Paderborn, Germany, pp: 314-319.

[8]Kedzier, M.A., Domanski, P.A., Generalized pressure drop correlation of evaporation and condensation in smooth and micro-fin tubes. In: Proc. IIR Conf., Commission B1, Paderborn, Germany, B4.9-B4.16.

[9]Oliver, J.A., Liebenberg, L. Pressure drop during refrigerant condensation inside horizontal smooth, helical microfin, and herringbone microfin tubes[J]. Heat Transfer, 2004, 126: 687-696.

[10] M. Goto, N. Inoue et al., Condensation and evaporation heat transfer of R410A inside internally grooved horizontal tubes[J]. International Journal of Refrigeration, 24(2001), pp 628-638.